Eur Biophys J (2010) 39:389–396
DOI 10.1007/s00249-009-0411-7

ORIGINAL PAPER

Phenomenological partial-specific volumes for G-quadruplex DNAs

Lance M. Hellman · David W. Rodgers · Michael Gregory Fried

Received: 26 November 2008 / Revised: 14 January 2009 / Accepted: 29 January 2009 / Published online: 24 February 2009

Abstract Accurate partial-specific volume ($\bar{v}$) values are required for sedimentation velocity and sedimentation equilibrium analyses. For nucleic acids, the estimation of these values is complicated by the fact that $\bar{v}$ depends on base composition, secondary structure, solvation and the concentrations and identities of ions in the surrounding buffer. Here we describe sedimentation equilibrium measurements of the apparent isopotential partial-specific volume ϕ' for two G-quadruplex DNAs and a single-stranded DNA of similar molecular weight and base composition. The G-quadruplex DNAs are a 22 nucleotide fragment of the human telomere consensus sequence and a 27 nucleotide fragment from the human c-myc promoter. The single-stranded DNA is 26 nucleotides long and is designed to have low propensity to form secondary structures. Parallel measurements were made in buffers containing NaCl and in buffers containing KCl, spanning the range 0.09 M $\leq$ [salt] $\leq$ 2.3 M. Limiting values of ϕ', extrapolated to [salt] = 0 M, were: 22-mer (NaCl-form), 0.525 $\pm$ 0.004 mL/g; 22-mer (KCl-form), 0.531 $\pm$ 0.006 mL/g; 27-mer (NaCl-form), 0.548 $\pm$ 0.005 mL/g; 27-mer (KCl-form), 0.557 $\pm$ 0.006 mL/g; 26-mer (NaCl-form), 0.555 $\pm$ 0.004 mL/g; 26-mer (KCl-form), 0.564 $\pm$ 0.006 mL/g. Small changes in ϕ' with [salt] suggest that large changes in counterion association or hydration are unlikely to take place over these concentration ranges.

AUC&HYDRO 2008—Contributions from 17th International Symposium on Analytical Ultracentrifugation and Hydrodynamics, Newcastle, UK, 11–12 September 2008.

L. M. Hellman · D. W. Rodgers · M. G. Fried (✉)
Department of Molecular and Cellular Biochemistry, Center for Structural Biology, University of Kentucky, 741 South Limestone, Lexington, KY 40536-0509, USA
e-mail: michael.fried@uky.edu

Keywords Partial-specific volume · Analytical ultracentrifugation · G-quadruplex DNA · Single-stranded DNA

List of symbols

$\bar{v}$	Partial-specific volume
ϕ'	Apparent partial-specific volume
$\phi'_{(E-S)}$	Apparent partial-specific volume determined by Edelstein–Schachman equation
$\phi'_{(avg)}$	Averaged apparent partial-specific volume
$\phi'_{(extrap)}$	Extrapolated apparent partial-specific volume to [salt] = 0 M
M_b	Buoyant molecular weight
M_{app}	Apparent molecular weight
$s_{T,B}$	Sedimentation coefficient at experimental temperature and buffer
$s_{20,w}$	Sedimentation coefficient at 20°C in water
f/f_0	Frictional ratio

Introduction

The ability of guanines to form G-tetrads was first proposed over 45 years ago (Gellert et al. 1962). The role of G-tetrad containing quadruplexes in maintaining the stability of chromosome ends was postulated approximately 25 years later (Henderson et al. 1987; Williamson et al. 1989). Today, G-quadruplex-containing telomere structures are known to be essential for the maintenance of linear chromosome structure (Greider and Blackburn 1985; Kang et al. 1992). Recently, G-quadruplexes have been proposed to function as a means for keeping promoter regions of various genes readily accessible to regulatory proteins (Lane et al. 2008).

Sedimentation methods are increasingly used for the characterization of structures containing nucleic acids, and accurate specification of the partial-specific volume ($\bar{v}$) is essential for calculation of molecular weights and frictional ratios from sedimentation data. However, beyond the classical single-stranded and duplex DNA structures (for which $\bar{v}$ values have been tabulated by Durchschlag (1986), relatively few nucleic acid secondary structures have been characterized in this way. The classical approach to measuring $\bar{v}$ involves the accurate measurement of solution densities at macromolecular concentrations sufficient to cause measurable change in solution density (Lee et al. 1979). This approach requires high concentrations of homogeneous macromolecule (typically in the range of 3–20 mg/mL) and highly-accurate densimetry (Lee et al. 1979; Durchschlag 1986). The quantities of macromolecule required by this approach have limited its use to stable, easily acquired specimens.

An alternate method offering accurate approximations of $\bar{v}$ and requiring smaller quantities of macromolecule, was developed by Edelstein and Schachman (1967, 1973). This approach uses sedimentation equilibrium measurement of buoyant molecular weights in H_2O and D_2O solutions of differing density. Here, we use a variation of the Edelstein–Schachman method, in which the solvent density is varied by changing the salt concentration. This variation depends on the assumption, justified by counterion–condensation theory (Manning 1978), that the fractional charge neutralization of nucleic acids by monovalent cations saturates at salt concentrations well below those typically used in analytical ultracentrifugation analysis. We also present an alternative approach, using known sequence molecular weights to calculate the apparent isopotential partial-specific volume (ϕ') directly from sedimentation equilibrium data. We use these methods to determine the ϕ' of two G-quadruplex structures, for which good experimental values of $\bar{v}$ or ϕ' do not exist, and of a single-stranded DNA, to provide a basis for comparing these methods with results obtained by classical densimetry.

The DNAs that we have chosen to study have different base compositions and secondary structures. Two (of 22 nt and 27 nt) have been shown to form G-quadruplex structures; one (a 26-mer) is designed to be largely single-stranded (Table 1). In addition, the G-quadruplex structures are likely to differ in secondary fold. As shown in Fig. 1a, the Na^+-form of the 22-mer has a structure with a single diagonal loop and two laterals, known as a "basket" conformation (PDB identifier 143D; Wang and Patel 1993). Under crystallization conditions, the K^+-form of the 22-mer can take on a conformation with a three-strand reversal that has no lateral loops, also called a "propeller" structure (PDB identifier 1KF1; Parkinson et al. 2002). However, in free solution, a 23-mer of the same sequence with an additional 5′ deoxythymidine residue folds to form a mixed "3 + 1" structure distinct from the propeller structure (PDB identifier 2JSM; Phan et al. 2007; Fig. 1c). There is evidence that the 22-mer sequence used in the studies described here also samples the "3 + 1" fold in K^+-solutions (Ambrus et al. 2006). It is noteworthy that the 3 + 1 structure also differs from the pure basket conformation that is seen with the Na^+-form (compare Fig. 1 panels a, c). In sodium and potassium solutions, the 22-mer forms three stacked G-tetrads connected by loops containing three un-paired nucleotides. The 27-mer also folds to form a "propeller" conformation in potassium-containing buffers (PDB identifier 1XAV; Ambrus et al. 2005). However, this sequence has five G-tracts that may participate in quadruplex structures. Since only four are needed to form a G-quadruplex, the 27-mer sequence has the potential to form several alternative folds. The number of nucleotides present in the loops depends on which G-tracts are used in the quadruplex. The lengths of unpaired 5′ and 3′ ends are also dependent on the G-tracts involved in structure formation and can reach lengths up to 7 or 9 nucleotides, respectively. To our knowledge there is no high-resolution structure available for the sodium form of the 27-mer, but hydrodynamic data shown below are consistent with the idea that its structure is different from that of the potassium form. Alternate possible structures of the 22-mer quadruplex DNA are contrasted in Fig. 1. Several factors contribute to partial-specific volume. Among these are residue composition, packing and solvent interactions including electrostriction (Durchschlag 1986). Since our DNA molecules have different folds and offer different surfaces for solvent interaction, we anticipated that they would have different partial-specific volumes. The experiments described below test that prediction.

Table 1 Oligonucleotide sequences

Length, bp	Sequence molecular weights (Da)	Sequence
22	6,967	5′-AGGGTTAGGGTTAGGGTTAGGG-3′
26	7,996	5′-AGTCAGTCAGTCAGTCAGTCAGTCAG-3′
27	8,688	5′-TGGGGAGGGTGGGGAGGGTGGGGAAGG-3′

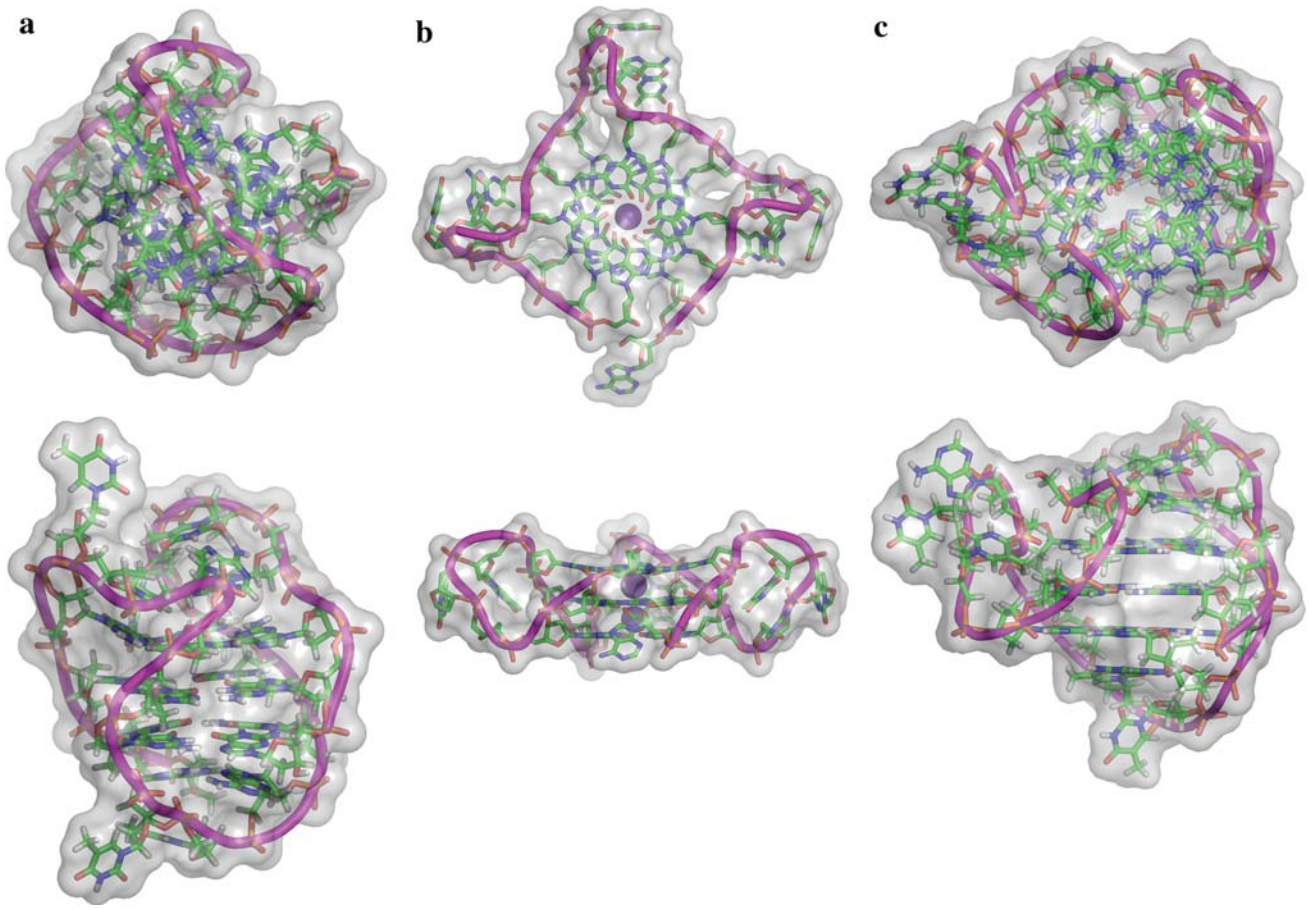

Fig. 1 Conformations of the 22-mer G-quadruplex DNA depend on cation identity. *Panel* (**a**): views of the structure of the Na^+-form of the 22-mer (PDB identifier 143D) determined by Wang and Patel (1993). This structure has a solvent-accessible surface area of 3,865 $Å^2$. The top image is an end-view of the molecule; the bottom image, a side-view. *Panel* (**b**): views of the propeller structure of the K^+-form of the 22-mer (PDB identifier 1KF1) determined by Parkinson et al. (2002). This structure has a solvent-accessible surface area of 4461 $Å^2$. The top image is an end-view of the molecule; the bottom image, a side-view. The central K^+ ions are represented by *purple spheres* (ionic radii reduced by half for clarity). *Panel* (**c**): views of the mixed "3 + 1" structure obtained for the K^+-form of the closely-related 23-mer (PDB identifier 2JSM) determined by Phan et al. (2007). The sequence of this molecule is the same as that of the 22-mer, with an additional deoxythymidine residue added at the 5′-end. This structure has a solvent-accessible surface area of 3,730 $Å^2$; a model calculation for this structure with the 5′ deoxythymidine removed gave a solvent-accessible surface area of 3,830 $Å^2$. The top image is an end-view of the molecule; the bottom image, a side-view. Backbone trajectories are indicated by *purple ribbons*. Approximate van der Waals surfaces are indicated by the *grey envelopes* surrounding each structure

Experimental

The sequences of the DNA molecules used are given in Table 1. These DNAs were obtained from Invitrogen and used without further purification. Aliquots of each sample were dialyzed against 10 mM Tris (pH 8.0), 1 mM EDTA (TE buffer), adjusted to contain a final concentration of 75 mM NaCl or KCl (as appropriate). Samples were heated to ~100°C for 1 min and allowed to slowly cool to 37°C and then annealed in a water-bath overnight at 37°C. Samples were dialyzed overnight at 4°C against TE buffer, adjusted to contain working concentrations of NaCl or KCl, as appropriate. After dialysis, buffers were thoroughly degassed and densities were measured using a Mettler DA-300 density meter at 4°C. For densimetry, temperature was controlled to ±0.01°C.

Analytical ultracentrifugation

Sedimentation velocity and equilibrium experiments were performed using a Beckman XL-A analytical ultracentrifuge. Sedimentation velocity experiments were performed at 4°C and 40,000 rpm. Absorbance measurements were made at 260 nm. Distributions of sedimentation coefficients $c(s)$ were determined using Sedfit (Schuck et al. 2002). Sedimentation equilibrium data were obtained at 4°C with rotor speeds spanning the range 20,000–45,000 rpm. Equilibrium was considered to be attained

when scans taken 6 h apart superimposed. Sedimentation equilibrium data were analyzed using Eq. 1.

$$A(r) = \sum_n \alpha_{n,0} \exp\left[\sigma_n\left(r^2 - r_0^2\right)/2\right] + \zeta \quad (1)$$

Here $A(r)$ is the absorbance at radial position r, $\alpha_{n,0}$ is the concentration of the nth species at radial position r_0, and $\sigma_n = M_n\left(1 - \phi_n'\rho\right)\omega^2 \Big/ RT$. M_n is the molecular weight of species n, ϕ_n' the apparent isopotential partial-specific volume of the nth species, ρ the solvent density, ω the angular velocity, R is the gas constant, T the absolute temperature, and ζ is a baseline offset term (Laue 1995).

The apparent partial-specific volume, ϕ', was measured by a variation the method of Edelstein and Schachman (1967, 1973), in which solvent densities are modulated by changing the salt concentration. In this analysis, ϕ'_{E-S} is given by the relation

$$\phi'_{(E-S)} = \frac{k - (Q_H/Q_L)}{\rho_H - \rho_L(Q_H/Q_L)} \quad (2)$$

Here k is the ratio of molecular weights under high density conditions (H) to that under low density conditions (L) Edelstein and Schachman (1967, 1973). Because DNA molecular weights are not expected to change with [salt], we set $k = 1$ for our analyses. Q is the integrated form of Eq. 1 for a single, ideal species.

$$Q = \frac{d\ln c}{dr^2} = \frac{M(1 - \phi'\rho)\omega^2}{2RT} \quad (3)$$

Here c is macromolecular concentration. This method allows the simultaneous determination of M and ϕ', but it requires data in which values of Q are constant within each experiment. Sources of deviation from a linear relationship of ln c with r^2 include macromolecular inhomogeneity and non-ideal sedimentation.

Because the sequence molecular weights of our DNAs are accurately known, an alternate, phenomenological estimate of ϕ' could be obtained by directly fitting sedimentation equilibrium data with Eq. 1, as originally described by Ebel et al. (2000). In this analysis M_n was input as a fixed value and ϕ' was allowed to float.

Structural calculations

Solvent-accessible surface areas were calculated by the Connolly method (Connolly 1983) using a probe of 1.4 Å radius, implemented in the program GRASP (Nicholls et al. 1991).

Results

Sedimentation velocity experiments were performed to determine the number of independently-sedimenting species in each DNA preparation and to determine whether the G-quadruplex DNAs were folded into compact secondary structures or whether they were present in unfolded, extended states. As shown in Fig. 2a, solutions of 22-mer

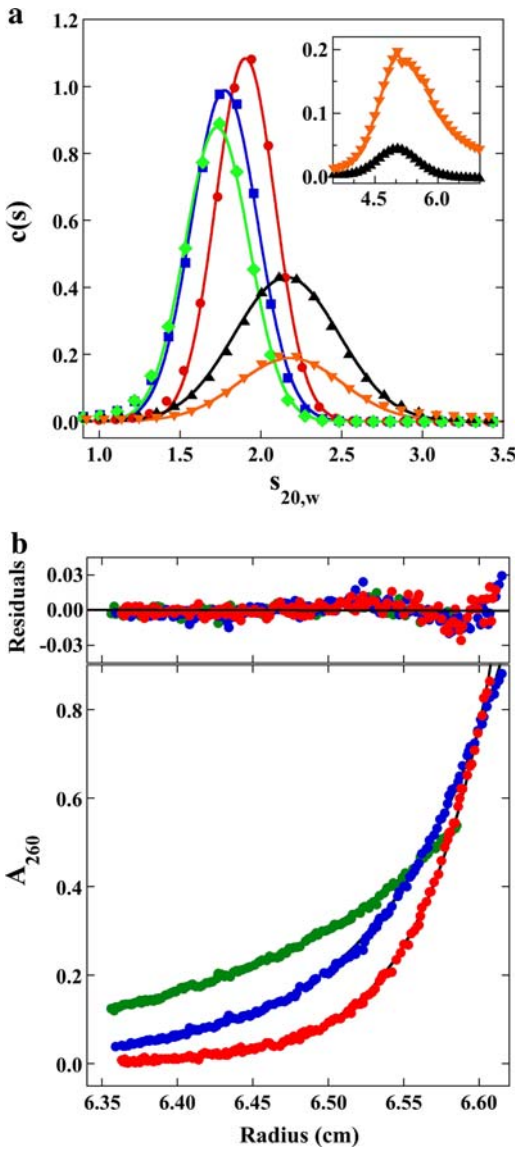

Fig. 2 Sedimentation analysis of DNAs. (a) Representative sedimentation velocity data at 40,000 rpm for 22-mer G-quadruplex DNA in 10 mM Tris (pH 8.0), 1 mM EDTA (TE buffer) containing 75 mM KCl (*red circles*); 22-mer G-quadruplex DNA in TE buffer containing 75 mM NaCl (*blue squares*); 26-mer ssDNA in TE buffer containing 75 mM NaCl (*green diamonds*); the 27-mer G-quadruplex DNA in TE buffer containing 75 mM NaCl (*black triangles*), and the 27-mer G-quadruplex DNA in TE buffer containing 75 mM KCl (*orange triangles*) by analytical ultracentrifugation. The $s_{20,w}$ values, with 95% confidence intervals indicated in parentheses were as follows. 22-mer (NaCl-form), 1.75 s (1.73–1.80); 22-mer (KCl-form), 1.88 s (1.85–1.93); 26-mer (NaCl-form), 1.72 s (1.67–1.73); 27-mer (NaCl-form); 2.10 s (1.94–2.16); and 27-mer (KCl-form), 2.17 s (2.12–2.46). (b) Representative sedimentation equilibrium data at 4°C for the 22-mer G-quadruplex DNA in TE buffer containing 0.4 M KCl at 25,000 (*green*), 35,000 (*blue*), and 45,000 rpm (*red*) by analytical ultracentrifugation. The *smooth curves* represent fits of Eq. 1 to the experimental data

Table 2 Sedimentation velocity data

DNA fragment	Buffer salt	$s^{a}_{T,B}$	$s^{b}_{20,w}$	M^{a}_{app} (Da)	f/f^{b}_{0}
22-mer	NaCl	1.10 (1.09–1.13)[c]	1.75 (1.73–1.80)[c]	6762 (6362–7024)[c]	1.42 (1.38–1.43)[c]
	KCl	1.19 (1.17–1.22)[c]	1.88 (1.85–1.93)[c]	7128 (6853–7383)[c]	1.33 (1.29–1.35)[c]
26-mer	NaCl	1.08 (1.05–1.09)[c]	1.72 (1.67–1.73)[c]	7622 (7372–7934)[c]	1.58 (1.56–1.62)[c]
	KCl	n/a	n/a	n/a	n/a
27-mer[d]	NaCl	1.32 (1.28–1.36)[c]	2.10 (2.04–2.16)[c]	8947 (8053–9747)[c]	1.37 (1.33–1.41)[c]
	KCl	1.33 (1.30–1.51)[c]	2.17 (2.12–2.46)[c]	7646 (6646–8746)[c]	1.33 (1.17–1.36)[c]

[a] Buffer viscosities and densities were determined using Sednterp (Laue et al. 1992); values were determined using Sedfit (Schuck et al. 2002)

[b] Buffer viscosities and densities along with $s_{20,w}$ and f/f_0 values were determined using Sednterp (Laue et al. 1992) with $\bar{\nu} = 0.54$ (Durchschlag 1989), and using sequence molecular weights (with two cations associated with the G-quadruplex DNAs)

[c] 95% confidence interval

[d] Slower sedimenting species

and 26-mer contained single sedimenting species but the 27-mer preparations contained two discrete species. Analysis of c(M) distributions (summarized in Table 2) indicate that the 22-mer and 26-mer species were monomeric, as was the most slowly-sedimenting species present in the 27-mer samples. The faster-sedimenting peak in the 27-mer samples had an apparent molecular weight consistent with a tetrameric structure.

As shown in Table 2, the $s_{20,w}$ values for the monomeric forms of 22-mer and 27-mer DNAs are larger than those of the single-stranded 26-mer, indicating that they are compactly folded. The value of $s_{20,w}$ for the 22-mer is similar to previously-reported values for the quadruplex structure of this DNA (Li et al. 2005; Mekmaysy et al. 2008). To our knowledge, the $s_{20,w}$ value for the single-stranded 26-mer sequence has not been reported. Differences in $s_{20,w}$ for G-quadruplex DNAs annealed in NaCl and KCl buffers are likely to signify differences in the compactness of these structures (Parkinson et al. 2002; Wang and Patel 1993).

To perform the Edelstein–Schachman analysis of ϕ', DNA samples were brought to sedimentation equilibrium at 4°C. Buffer densities were varied by changing [NaCl] or [KCl]. Equilibrium data from the 22-mer G-quadruplex DNA (Fig. 2b) and the 26-mer ssDNA were consistent with a single species for each preparation, however, data for the 27-mer could not be fit with the version of Eq. 1 that describes a single species. Consistent with the sedimentation velocity result (Fig. 2a), an additional term with buoyant molecular weight approximately 4-times that of monomer was needed to account for the sedimentation equilibrium distribution of samples of 27-mer (result not shown). For the homogeneous samples obtained with 22-mer and 26-mer DNAs, values of Q were calculated using Eq. 3. Graphs of Q as functions of [salt] and solution density, for NaCl and KCl solutions are shown in Fig. 3. Values of ϕ'_{E-S} were calculated from the density dependence of Q, using Eq. 2. For the quadruplex 22-mer in

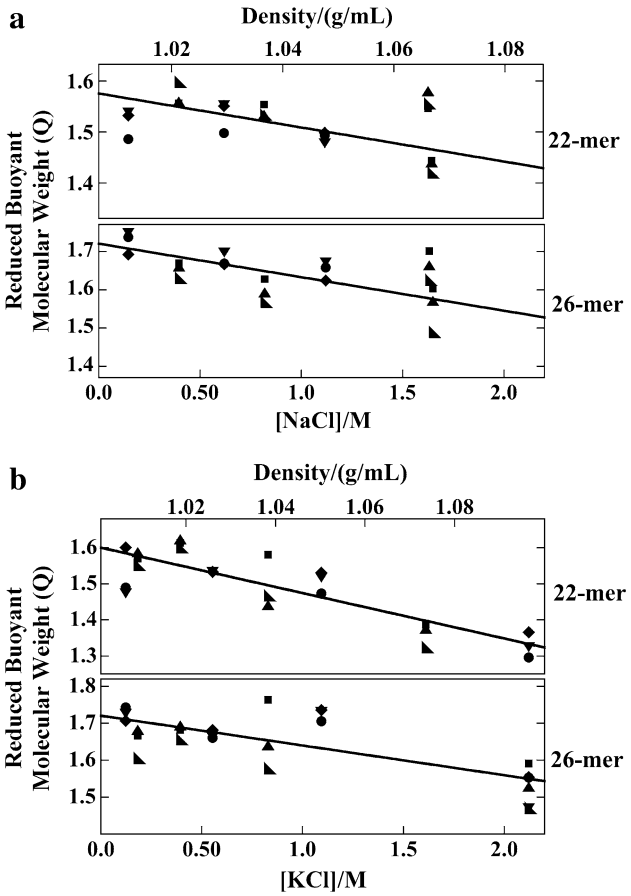

Fig. 3 Determination of partial-specific volume by the method of Edelstein and Schachman. Graphs of reduced buoyant molecular weight (Q) as a function of solvent density. (a) Samples brought to sedimentation equilibrium in TE buffer, with indicated concentrations of NaCl. (b) Samples brought to sedimentation equilibrium in TE buffer, with indicated concentrations of KCl. *Solid lines* are least squares fits from which the Q_H/Q_L ratios were determined

NaCl and KCl buffers values of ϕ'_{E-S} were 0.574 ± 0.090 and 0.588 ± 0.088 mL/g, respectively and the corresponding values for the 26-mer in NaCl and KCl were

Table 3 Comparison of partial-specific volume calculations

DNA fragment	Salt	$\phi'_{(E-S)}$ (mL/g)	$\phi'_{(avg)}$ (mL/g)	$\phi'_{(extrap)}$ (mL/g)
22-mer	NaCl	0.574 ± 0.090	0.536 ± 0.009	0.525 ± 0.004
	KCl	0.588 ± 0.088	0.541 ± 0.019	0.531 ± 0.006
26-mer	NaCl	0.525 ± 0.028	0.548 ± 0.021	0.555 ± 0.004
	KCl	0.590 ± 0.057	0.551 ± 0.015	0.564 ± 0.006
27-mer	NaCl	n/a	0.546 ± 0.005	0.548 ± 0.005
	KCl	n/a	0.556 ± 0.013	0.557 ± 0.006

$\phi'_{(E-S)}$ are calculated from Q using Eq. 3

$\phi'_{(avg)}$ are values of $\phi'_{(E-S)}$ averaged over the experimental [salt] range

$\phi'_{(extrap)}$ are obtained by linear extrapolation of $\phi'_{(E-S)}$ to [salt] = 0 M

0.525 ± 0.028 and 0.590 ± 0.057 mL/g, respectively (Table 3). As discussed below, these values and their ranges overlap with ones obtained by direct fitting of ϕ' using Eq. 1 and the sequence molecular weights of the DNAs. Because samples containing the 27-mer were heterogeneous, the dependence of ln c on r^2 was non-linear and unique values of Q could not be obtained at any salt concentration. This prevented estimation of ϕ' for the 27-mer quadruplex by the Edelstein–Schachman method.

Phenomenological values of ϕ' were obtained by fitting equilibrium data using Eq. 1, with M_n fixed, but adjustable ϕ', as originally described by Ebel et al. (2000). G-quadruplex structures are stabilized by a single tightly-bound cation located in the center of each G-quartet or between two G-quartet planes (Burge et al. 2006). Our calculations used values of M_n that assumed two non-exchanging cations per quadruplex-forming DNA molecule; if these sites were unoccupied, this would result in errors in M_n of ≤1.1%. This translates into an error in ϕ' of ∼0.5%. This uncertainty is comparable to the uncertainty in ϕ' due to experimental scatter. Data was obtained over salt concentration ranges 0.09 M ≤ [NaCl] ≤ 2.3 M and 0.09 M ≤ [KCl] ≤ 2.1 M (Fig. 4); over these ranges, the apparent change in ϕ' with salt concentration is less than the scatter of data. The small dependence of ϕ' values on salt concentration is inconsistent with large, [salt] dependent conformational changes, while the absence of large changes in $M_n(1 - \phi'\rho)$ is inconsistent with the formation of new quaternary interactions or increases in molecular weight due to counterion binding. These results are compatible with the prediction that cation binding to oligoelectrolytes with charge densities like that of DNA, dissolved in 1:1 salt solutions, saturates at low

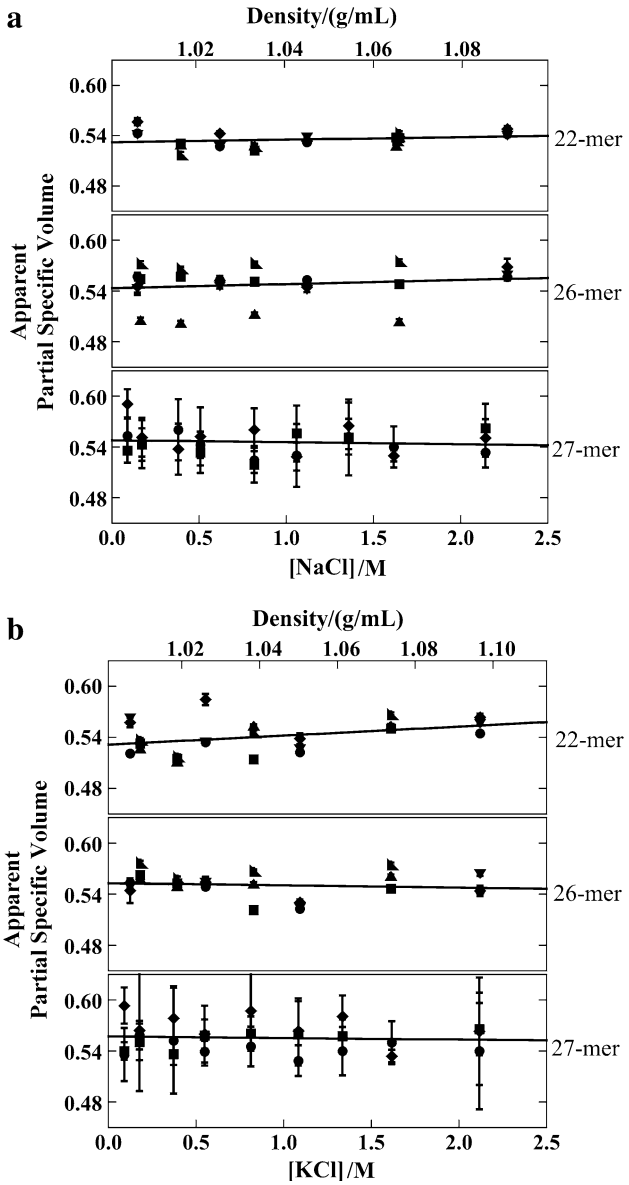

Fig. 4 Partial-specific volumes estimated from sequence molecular weights. (a) Graph of apparent partial-specific volumes as functions of NaCl concentration and solution density (ρ). Symbols: (*filled circle*) data acquired at 20,000 rpm; (*filled square*) data acquired at 25,000 rpm; (*filled diamond*) data acquired at 30,000 rpm; (*filled triangle*) data acquired at 35,000 rpm; (*filled inverted triangle*) data acquired at 40,000 rpm; (*filled rightangle*) data acquired at 45,000 rpm. All symbols have *error bars* representing 95% confidence intervals; where they cannot be seen, the interval is smaller than the size of the data symbol. The *solid line* is a linear fit to the data. Extrapolation to [NaCl] = 0 M provides a [salt]-independent reference value of ϕ'. Limiting values are as follows: 22-mer, 0.525 ± 0.004 mL/g; 26-mer, 0.555 ± 0.004 mL/g; 27-mer, 0.548 ± 0.005 mL/g. (b) Graph of apparent partial-specific volumes as functions of KCl concentration and solution density (ρ). Symbols: (*filled circle*) data acquired at 20,000 rpm; (*filled square*) data acquired at 25,000 rpm; (*filled diamond*) data acquired at 30,000 rpm; (*filled triangle*) data acquired at 35,000 rpm; (*filled inverted triangle*) data acquired at 40,000 rpm; (*filled rightangle*) data acquired at 45,000 rpm. All symbols have *error bars* representing 95% confidence intervals; where they cannot be seen, the interval is smaller than the size of the data symbol. The *solid line* is a linear fit to the data. Limiting values at [KCl] = 0 M are: 22-mer, 0.531 ± 0.006 mL/g; 26-mer, 0.564 ± 0.006 mL/g; 27-mer, 0.557 ± 0.006 mL/g

millimolar salt concentrations (Manning 1978). Average values of ϕ' for the 22-mer G-quadruplex in NaCl and KCl buffers were 0.536 ± 0.009 and 0.541 ± 0.019 mL/g; for the 26-mer ssDNA, 0.548 ± 0.021 and 0.551 ± 0.015 mL/g; and for the 27-mer G-quadruplex, 0.546 ± 0.005 mL/g and 0.556 ± 0.013 mL/g, respectively. As a result of the very small dependence of on [salt], values of ϕ' extrapolated to [salt] = 0 M are virtually indistinguishable from the average values (Table 3).

Discussion

The Edelstein–Schachman method is useful for the determination of ϕ' with homogeneous solutes in two- or three-component systems. In the variant of the method used here, we have altered solvent density by changing salt concentration. This relies on the assumption that factors affecting partial-specific volume will be, to a first approximation, independent of [salt] over the range of concentrations that we have tested. The linear dependences of Q and ϕ' on [salt] (Figs. 3 and 4) show this to be the case. We note that our experiments do not extend into the low-salt range in which the partial-specific volumes of nucleic acids are highly-dependent on salt concentration (c.f. Durchschlag 1989). The Edelstein–Schachman approach requires a linear dependence of ln c on r^2 (Eq. 3), which is not always observed for heterogeneous macromolecular systems. The alternate approach, in which ϕ' is calculated from buoyant molecular weight data and the sequence molecular weight, does not have this drawback because values are obtained by direct fitting of Eq. 1 and because the determination does not involve the accurate measurement of differences in a parameter such as Q, as a function of solvent density. However, we emphasize that this approach to estimating ϕ' requires accurate prior knowledge of the sequence molecular weight.

The single-stranded and G-quadruplex DNAs that we have studied have different secondary structures, different solvent-accessible surface areas and different numbers and kinds of ion-binding sites. Thus it is remarkable that the values of ϕ' and $\phi'_{(E-S)}$ obtained for 22, 26 and 27 nt DNAs, in sodium and potassium buffers are so similar to one another (Table 3). We rationalize this as follows. While the base compositions of the 22, 26 and 27 nt DNAs differ, so do the proportions of bases that are stacked and the proportions that are engaged in hydrogen-bonded pairs or quartets. In addition, the relative amounts of charged and uncharged and polar and non-polar surface exposed to solvent differ from molecule to molecule and between conformations of the same molecule. These differences may exert compensating effects resulting in the small range in ϕ' values that we have observed.

The quadruplex-forming molecules that we have tested are mixtures of G-quartet, loop and single-stranded motifs; each is expected to contribute to the value of ϕ' observed for that molecule and conformation. Thus, these experiments do not establish a value of ϕ' for a pure G-quartet structure, although they provide values for quadruplex-containing structures that may be biologically-relevant. The values of ϕ' that we observe for G-quadruplex DNAs are similar to ones reported for populations of multimers of dG_8 and dG_{16} ($\phi' \sim 0.54$ mL/g) that were likely to contain quadruplex structures (Hatters et al. 2001). The values of ϕ' obtained for the single-stranded 26-mer are the same, within-error, as that measured for a different single-stranded DNA by Chapman and Sturtevant (1969) and cited more recently (Durchschlag 1986).

It is striking that values of ϕ' do not depend significantly on the identity of the dominant buffer cation for any of the DNAs that we have sampled. This is particularly intriguing in view of the range of different quadruplex folds observed for the 22-mer DNA in sodium and potassium buffers (Fig. 1) and the fact that both 22-mer and 27-mer quadruplex DNAs undergo shifts in hydrodynamic properties with cation substitution (Fig. 2a; Table 2). The data obtained for single-stranded DNA indicates that the insensitivity of ϕ' to cation substitution is not a unique property of quadruplex-containing DNAs. Finally, the values of ϕ' for single-stranded and G-quadruplex DNAs fall within the range observed for duplex DNA at comparable salt concentrations ($0.503 \leq \phi' \leq 0.579$ mL/g; Cohen and Eisenberg, 1968; Bonifacio et al. 1997). Given the range of secondary structures spanned by our data and that in the literature, we conclude that at moderate salt concentrations, ϕ' is at most weakly dependent on the amount and kind of secondary structure that is present in a DNA sample.

References

Ambrus A, Chen D, Dai J, Jones RA, Yang D (2005) Solution structure of the biologically relevant G-quadruplex element in the human c-MYC promoter. Implications for G-quadruplex stabilization. Biochemistry 44:2048–2058. doi:10.1021/bi048242p

Ambrus A, Chen D, Dai J, Bialis T, Jones RA, Yang D (2006) Human telomeric sequence forms a hybrid-type intramolecular G-quadruplex structure with mixed parallel/antiparallel strands in potassium solution. Nucleic Acids Res 34:2723–2735. doi:10.1093/nar/gkl348

Bonifacio GF, Brown T, Conn GL, Lane AN (1997) Comparison of the electrophoretic and hydrodynamic properties of DNA and RNA oligonucleotides duplexes. Biophys J 73:1532–1538. doi:10.1016/S0006-3495(97)78185-2

Burge S, Parkinson GN, Hazel P, Todd AK, Neidle S (2006) Quadruplex DNA: sequence, topology and structure. Nucleic Acids Res 34:5402–5412. doi:10.1093/nar/gkl655

Chapman RE Jr, Sturtevant JM (1969) Volume changes accompanying the thermal denaturation of deoxyribonucleic acid I.

Denaturation at neutral pH. Biopolymers 7:527–537. doi:10.1002/bip.1969.360070410

Cohen G, Eisenberg H (1968) Deoxyribonucleate solutions: sedimentation in a density gradient, partial specific volumes, density and refractive index increments, and preferential interactions. Biopolymers 6:1077–1100. doi:10.1002/bip.1968.360060805

Connolly ML (1983) Solvent-accessible surfaces of proteins and nucleic acids. Science 221:709–713. doi:10.1126/science.6879170

Durchschlag H (1986) Specific volumes of biological macromolecules and some other molecules of biological interest. In: Hinz H-J (ed) Thermodynamic data for biochemistry and biotechnology, chapter 3. Springer, New York, pp 45–128

Durchschlag H (1989) Determination of the partial specific volume of conjugated proteins. Colloid Polym Sci 267:1139–1150. doi:10.1007/BF01496937

Ebel C, Eisenberg H, Ghirlando R (2000) Probing protein–sugar interactions. Biophys J 78:385–393. doi:10.1016/S0006-3495(00)76601-X

Edelstein SJ, Schachman HK (1967) The simultaneous determination of partial specific volumes and molecular weights with microgram quantities. J Biol Chem 242:306–311

Edelstein SJ, Schachman HK (1973) Measurement of partial specific volume by sedimentation equilibrium in H_2O–D_2O solutions. Methods Enzymol 27:82–98. doi:10.1016/S0076-6879(73)27006-4

Gellert M, Lipsett MN, Davies DR (1962) Helix formation by guanylic acid. Proc Natl Acad Sci USA 48:2013–2018. doi:10.1073/pnas.48.12.2013

Greider CW, Blackburn EH (1985) Identification of a specific telomere terminal transferase activity in *Tetrahymena* extracts. Cell 43:405–413. doi:10.1016/0092-8674(85)90170-9

Hatters DM, Wilson L, Atcliffe BW, Mulhern TD, Guzzo-Pernell N, Howlett GJ (2001) Sedimentation analysis of novel DNA structures formed by homo-oligonucleotides. Biophys J 81:371–381. doi:10.1016/S0006-3495(01)75706-2

Henderson E, Hardin CC, Walk SK, Tinoco I, Blackburn EH (1987) Telomeric DNA oligonucleotides form novel intramolecular structures containing guanine–guanine base pairs. Cell 51:899–908. doi:10.1016/0092-8674(87)90577-0

Kang C, Zhang X, Ratliff R, Moyzis R, Rich A (1992) Crystal structure of four-stranded *Oxytricha* telomeric DNA. Nature 356:126–131. doi:10.1038/356126a0

Lane AN, Chaires JB, Gray RD, Trent JO (2008) Stability and kinetics of G-quadruplex structures. Nucleic Acids Res 36:5482–5515. doi:10.1093/nar/gkn517

Laue TM (1995) Sedimentation equilibrium as thermodynamic tool. Methods Enzymol 259:427–452. doi:10.1016/0076-6879(95)59055-2

Laue TM, Shah BD, Ridgeway TM, Pelletier SL (1992) Computer-aided interpretation of analytical sedimentation data for proteins. In: Harding SE, Rowe AJ, Harding JC (eds) Analytical ultracentrifugation in biochemistry and polymer science. The Royal Society of Chemistry, Cambridge, England, pp 90–125

Lee JC, Gekko K, Timasheff SN (1979) Measurements of preferential solvent interactions by densimetric techniques. Methods Enzymol 61:26–49. doi:10.1016/0076-6879(79)61005-4

Li J, Correia JJ, Wang L, Trent JO, Chaires JB (2005) Not so crystal clear: the structure of the human telomere G-quadruplex in solution differs from that present in a crystal. Nucleic Acids Res 33:4649–4659. doi:10.1093/nar/gki782

Manning GS (1978) Molecular theory of polyelectrolyte solutions with application to electrostatic properties of polynucleotides. Q Rev Biophys 11:179–246

Mekmaysy CS, Petraccone L, Garbett NC, Ragazzon PA, Gray R, Trent JO, Chaires JB (2008) Effect of O^6-methylguanine on the stability of G-quadruplex DNA. J Am Chem Soc 130:6710–6711. doi:10.1021/ja801976h

Nicholls A, Sharp KA, Honig B (1991) Protein folding and association: insights from the interfacial and thermodynamic properties of hydrocarbons. Proteins 11:281–296. doi:10.1002/prot.340110407

Parkinson GN, Lee MPH, Neidle S (2002) Crystal structure of parallel quadruplexes from human telomeric DNA. Nature 417:876–880. doi:10.1038/nature755

Phan AT, Kyryavyi V, Luu KN, Patel DJ (2007) Structure of two intramolecular G-quadruplexes formed by natural human telomere sequences in K^+ solution. Nucleic Acids Res 35:6517–6525. doi:10.1093/nar/gkm706

Schuck P, Perungini MA, Gonzales NR, Howlett GJ, Schubert D (2002) Size-distribution analysis of proteins by analytical ultracentrifugation: strategies and application to model systems. Biophys J 82:1096–1111. doi:10.1016/S0006-3495(02)75469-6

Wang Y, Patel DJ (1993) Solution structure of the human telomeric repeat $d[AG_3(T_2AG_3)_3]$ G-tetraplex. Structure 1:263–282. doi:10.1016/0969-2126(93)90015-9

Williamson JR, Raghuraman MK, Cech TR (1989) Monovalent cation-induced structure of telomeric DNA: the G-quartet model. Cell 59:871–880. doi:10.1016/0092-8674(89)90610-7